Impact of Reinforcing Additives on the Structure and Performance of Composite Films Based on Regenerated Cellulose from Corn Stalk Pith

Heng Zhang,[a,b] Quanqing Han,[a] Xin Gao,[a,b,*] Xiaoning Tang,[a,*] Keli Chen,[a] and Meng Li [a]

Cellulose was extracted from corn stalk pith (CSP) and used for fabricating hybrid composite films with acceptable physical properties. As reinforced additives, low contents of graphene oxide (GO) and black phosphorene (BP), both ranging from 0.05 to 0.15 wt%, were separately incorporated into the cellulose matrix in a $ZnCl_2$ aqueous system. A series of the composites were prepared *via* a regeneration process. The as-prepared composites showed various properties depending largely on the additive content, manner of processing, and the type of additive used. GO and BP nanosheets were homogeneously dispersed in the regenerated cellulose (RC), smoothly forming the dense films. Crystalline structures of RC-based films were revealed to be cellulose-II, and in addition to GO-crosslinked RC samples (RC-GO), an increase in the additive dosage led to a decrement in the crystallinity index of blended films (RC/GO and RC/BP). At 0.15 wt% additive amount, the RC-GO possessed superior thermal stability, tensile strength, and Young's modulus, increasing 7.8%, 190.2%, and 79.0%, respectively, while the RC/BP exhibited a 3.5 times improvement in the elongation at break.

Keywords: Composite film; Regenerated cellulose; Corn stalk pith; Graphene oxide; Black phosphorene

*Contact information: a: Faculty of Chemical Engineering, Kunming University of Science and Technology, Kunming 650500, Yunnan, China; b: Key Laboratory of Pulp and Paper Science and Technology of Ministry of Education/Shandong Province, Qilu University of Technology (Shandong Academy of Sciences), 250353, Jinan, China; *Corresponding authors: drgaoxin@sina.com; tangxn6666@sina.com*

INTRODUCTION

In recent years, there have been increased efforts to utilize non-petroleum-based polymers from sustainable and renewable resources due to the environmental dilemma. Therefore, researchers have paid much attention to exploit various bio-based composites with low environmental and safety risks. In fact, lignocellulosic sources from renewable biomass, such as agriculture crop waste, provide a good pathway to develop green materials. As agricultural waste, corn stalk is one of the most readily available crop residues and makes up almost 50% of the total agro-wastes in China (Lv *et al*. 2013). Although the core portion of corn stalk is obviously higher than the rind, the core pith has limited usage compared to the rind fibre, because it is made up of mainly parenchyma cells and marginally short fibres. The considerable annual output of corn core should be considered as an important resource. Because the core contains up to 35 wt% of cellulose (Zhang *et al*. 2018), it has potential to become a more valuable source than simply burning or it being discarded in farmland.

To exploit the full potential of cellulose, especially in the area of film manufacture, several solvent systems have been employed for dissolving and processing cellulose.

Concentrated zinc chloride salt ($ZnCl_2$) hydrate melt is a well-arranged class of melt complexes, and its ability for cellulose dissolution has been well-known and mentioned in several articles (Sen *et al*. 2016; Fan *et al*. 2018). They have many attractive advantages, such as recyclability, high dissolving efficacy, no pollution, low cost, and environmental friendliness, thus promising widespread applications on the industrial scale (Xu *et al*. 2016). All types of cellulose-based materials, including composites and films, have been produced successfully (Grinshpan *et al*. 1989; Schestakow *et al*. 2016) *via* the use of $ZnCl_2$ as the solvent. The $ZnCl_2$ solvent has offered convenient and multiple platforms for the fabrication of novel cellulose materials.

The main disadvantage of regenerated-cellulose (RC) film from stalk parenchyma cells is unfavourable mechanical properties. Hence, there have been numerous studies to enhance the physical properties of biofilms *via* incorporation of inorganic additives and/or crosslinking agents (Ammar *et al*. 2016; Garavand *et al*. 2017). As a functional derivative of graphene, GO possesses a large surface area and a variety of hydrophilic groups, including –COOH, -OH, -O-, and C=O. These functional groups improve the interfacial interaction between the GO and cellulose matrix. This facilitates the stress transfer from the natural polymer matrix to GO, which contribute to the apparent reinforcement of the composite films. Similar to graphene, black phosphorus (BP) has been rediscovered as a promising new two-dimensional material due to its acceptable Young's modulus, superior tensile strain, and flexibility (Khandelwal *et al*. 2017). The successful exfoliation of BP to few-layer BP or phosphorene has opened a new research field for studying the properties of phosphorus-based materials. Recently, the reference of Hanlon *et al*. 2015 has established that BP-related materials possess great potential as a reinforcing additive.

Although there have been reports of GO as a filler in the preparation of cellulosic films, little attention has been given to GO as a chemical crosslinking reagent to achieve desirable mechanical characteristics of the films. Besides, BP applications for the reinforcement of biomass films has not been fully developed yet. Due to their possessions of abundant functional groups (GO) and unique structures (GO and BP), a remarkable performance of the films should be produced. Herein, the RC film reinforced with GO or BP were prepared in order to comparatively research the properties of BP- and GO-doped nanocomposites and the impact of different treatment pathways on these two strength additives in the films. As far as the authors know, there have not been other significant studies of the importance of non-fibrous cellulose as a matrix in biofilms. Thus, the parenchyma cellulose, isolated from corn pith, was used for preparing a RC film via a $ZnCl_2$ aqueous solution. The main objectives of this study are to make a comparative study about the effects of GO and BP additions on the properties of the resulting products, and investigate how they improved the mechanical reinforcement.

EXPERIMENTAL

Materials

The corn stalks were collected from a farm in Yunnan, China. Bulk BP was kindly provided by the Key Laboratory of Phosphorus Chemical Engineering at Kunming University of Science and Technology (Yunnan, China). Analytical grade zinc chloride (purity ≥ 98%) was freeze-dried overnight for the removal of residual water prior to use, GO, glycerine, sodium chlorite, and all other chemicals, were purchased from Aladdin

Reagent Co., Ltd. (Shanghai, China) and used without further purification. Deionized water was used throughout this work.

Processing

Pre-treatments of BP and GO

The bulk BP (12.5 mg) was placed in a 50 mL centrifuge tube, mixed with deoxygenated water (25 mL), and purged with ultrahigh-purity argon for 3 min. Then, the BP slurry was subjected to ultrasonic stimulus under the conditions of 25 kHz and 900 W for 60 min at 22 °C (JY92-II D type disrupter; Ningbo Xin Zhi Science and Equipment Institute, Ningbo, China). The BP was dispersed into water forming a back suspension after repeating the above process 8 to 10 times. The few-layer BP dispersion at approximately 0.05 wt% was frozen by pouring liquid nitrogen into the sample tube, and freeze-dried to remove water. The dried product was stored under vacuum for the subsequent use.

The GO was pretreated in the deionized water at the consistency of approximately 0.1 g/L, and then agitated in a homogeneous disperser (ULTRA-TURRAX® Tube Drive Control; IKA, Staufen, Germany) at 5000 rpm for 6 h. Afterwards, the dispersed suspension was disrupted by ultrasonic irradiation with the same conditions as mentioned above for BP, until a luminously yellow suspension was achieved. Finally, the GO suspension was stored in a refrigerator at 4 ℃ for further use.

Preparation of regenerated cellulose/inorganic additives nanocomposite films

The corn core was milled to pass through a 40-mesh screen. Lignin was then removed from the corn core powder using an acidified sodium chlorite solution (0.9 wt%) at 75 °C for 1 h; this process was repeated four times until the product became white. Next, the delignified samples were treated with 5 wt% potassium hydroxide at 25 °C for 10 h to leach hemicellulose and pectin. Afterwards, the slurry was filtered and rinsed with deionized water repeatedly to make it neutral, and then the consistency of the samples was adjusted to 5 wt% for the next chemical process. The carboxyl content and degree of polymerization (DP) of the obtained cellulose were 0.92 mmol/g and 425, respectively.

To obtain composite films, the cellulose slurry was mixed with a 65 wt% solution of oven-dried $ZnCl_2$ powder, and the whole mixture was heated at 80 ± 0.1 °C in a water bath for 2 h. After the full swelling of the parenchyma cellulose, the GO suspension (or BP powder) was slowly dispersed into the above mixture under constant stirring for 30 min. Then, 5% (w/total fluid in the reaction) glycerine was added as plasticizer to the reaction system and continually agitated for another 30 min. At the end, the aqueous mixture containing the cellulose/inorganic additives slurry was transferred to a polytetrafluoro-ethylene utensil with a film thickness in the range of 0.09 mm to 0.15 mm. The utensil was immediately placed in an electrically-heated oven at 85 °C to dissolve the cellulose, blending the GO (or BP), and thus forming a gelatinous sheet. After being heated for 45 min, the jelly composite from the polytetrafluoroethylene utensil was then immersed in a deionized water bath to regenerate the cellulose, the film was detached, and excess chemicals were removed. A subset of parenchyma cellulose/GO (or BP) films were dried in a sheet machine dryer (No. 2547; KRK, Hiroshi, Japan), then conditioned (24 °C, 48 h, relative humidity of 50%) in an environmental chamber (LRH-250-HS; Huruiming Instruments Co., Ltd., Guangzhou, China) before use. The composite films are hereinafter referred to as RC/GO (or BP) X, with X being the additive (GO or BP) contents (in wt%) on a dry cellulose basis. To compare the results, a control sample (without GO or BP) whose DP value was approximately 373, was also fabricated following the same method.

For the preparation of GO-crosslinked RC film, the cellulose pulp with a certain amount of GO and glycerine was casted into the similar utensil and dried at 85 °C for 45 min. The resulting gel-like slice was cured at 140 °C for 5 min to achieve crosslinking. The other steps of the film realization were followed using the procedures described above. The GO-crosslinked RC samples were labelled as RC-GO X, where X is the weight ratio (wt%) of GO additive in parenchyma cellulose.

Characterization

Fourier transform infrared spectroscopy (FTIR) studies were conducted using a Vertex 70 FTIR spectrophotometer (Bruker, Billerica, MA, USA). All of the film samples were analyzed *via* the attenuated total reflection method without KBr addition. The spectra were recorded in reflection mode under the wavenumber range of 4000 cm^{-1} to 600 cm^{-1}.

Scanning electron microscopic (SEM) observation of the regenerated films was conducted using a Nova Nanosem 450 scanning electron microscope (Field Electron and Ion Company, Hillsboro, OR, USA) at an accelerating voltage of 5.0 kV. The samples were placed onto a carbon disk attached to the stage. The samples for SEM observation were chosen randomly from the films.

The crystalline phases of the samples were determined by X-ray diffraction (XRD) measurements on an X'Pert3 powder diffractometer (PANalytical Co., Ltd., Almelo, Netherlands). The samples were prepared by pressing the powder on a Si slide to flatten. Radial scans of intensity were recorded at ambient conditions over scattering 2θ angles from 5° to 50° (step size = 0.01313°, scanning rate = 13.77 s/step) by using a Cu Kα radiation (λ = 1.5406 Å), an operating voltage of 40 kV, and a filament current of 40 mA.

Thermogravimetric analysis (TGA) of films was performed using a Netzsch STA 449 F3 (Netzsch Scientific Instruments Trading Ltd., Selb, Germany). Thermograms of the samples were recorded between room temperature and 600 °C at a heating rate of 10 °C/min in an inert atmosphere maintained by a nitrogen flow of 50 mL/min.

The mechanical properties of the RC and hybrid films were evaluated using a tensile testing machine DRK 101 (Jinan Drick Insrument Co., Ltd., Jinan, China). The film was tested in accordance with the standard method ASTM D882-97 (1999). The machine was fitted with a 200-N load cell with a crosshead speed of 20 mm/min, and the initial distance between the grips was kept at 100 mm. The sample was cut into 15-mm-wide strips using a sharp razor blade. At least five specimens of each formulation were tested, and the corresponding average values were calculated. All of the measurements were performed under room temperature.

RESULTS AND DISCUSSION

Fabrication of RC-based Composite Films

The parenchyma cellulose isolated from corn stalk core showed a typically translucent flake-like shape and rough surface (Fig. 1a), which in turn contributed to its higher specific area of approximately 12.5 m^2/g compared with fibrous ones. This unique characteristic was convenient for solvent molecules to penetrate into the cellulose matrix and subsequently disrupt its recalcitrant structures. The mechanism of $ZnCl_2$ dissolution for solubilizing cellulose depends on the direct interaction of cellulose hydroxyl groups with $ZnCl_2$-hydrates ($[Zn(H_2O)_x][ZnCl_4]$). In the initial parenchyma cellulose-$ZnCl_2$ solution, the dissolved $ZnCl_2$ was present as hydrated zinc ions, with the water molecules

tightly bound to the inner coordination sphere of the Zn^{2+} cation (Fu *et al*. 2015). The $[Zn(H_2O)_x]^{2+}$ could form strong hydrogen bonding with cellulose to break the intermolecular hydrogen bonds (Sen *et al*. 2016). Additionally, the large steric hindrance of $[Zn(H_2O)_x][ZnCl_4]$ increased the distance between the polymer chains. During the coagulation process, the precursor $[Zn(H_2O)_x][ZnCl_4]$ converted into $ZnCl_2$ crystals, and the strong interchain interactions of the exposed chains resulted in the rapid self-aggregation of cellulose. The BP exhibited microribbon-like morphology with the thickness of several hundred nanometers, indicating its few-layer structure (Fig. 1b). The GO in this study exhibited extremely thin sheets with a folded feature (Fig. 1c). The even mass dispersion of GO and BP in the RC matrix increased from the initial wettability and subsequent hydrogen bonding that occurred between the oxygen functionalities of the two additives and cellulose. Furthermore, both the cellulose and GO contain essentially a large amount of carboxyl and hydroxyl groups, which would make it possible to form crosslinking bonds between them *via* esterification. Meanwhile, the zinc chloride hydrate discussed above is an acidic solvent due to both the Lewis acidity of the Zn^{2+} and the Brønsted acidity of the coordinated water (Sen *et al*. 2016), which reasonably might provide active catalyst media for RC-GO esterification.

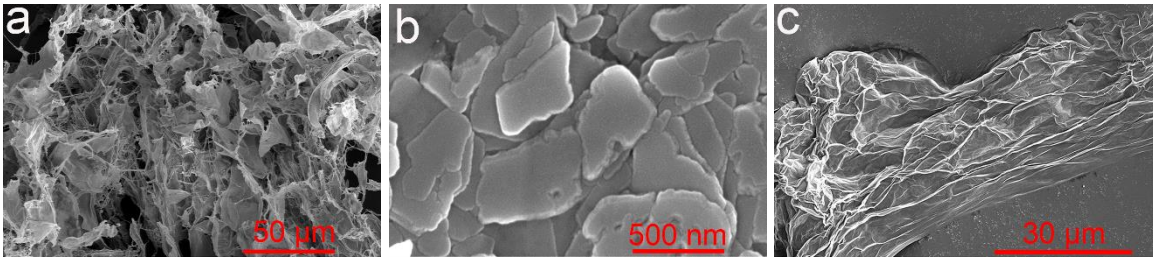

Fig. 1. SEM images of parenchyma cellulose (a), few-layer BP (b) and GO sheet (c)

Chemistry Characterization

Figure 2 shows the characteristic bands of the parenchyma cellulose found at 3400 cm^{-1} and 2900 cm^{-1}, which can be attributed to the hydroxyl stretching vibration and C-H stretching mode of the methyl group from cellulose, respectively (Gao *et al*. 2014). The adsorption peak at 1650 cm^{-1} is assigned to the H-O-H stretching vibration of absorbed water in cellulose, and the absorbance at 1022 cm^{-1} was due to the C-O-C pyranose ring skeletal vibrations (Gao *et al*. 2018). The presence of a sharp band at 1710 cm^{-1} confirmed the presence of carboxylic groups, which might explain why the oxidation reaction of cellulose somewhat occurred during the isolation process by the acidified sodium chlorite system. When BP was blended with the RC, the intensity of the peak at 3400 cm^{-1} visibly deceased with an increase of BP addition in the RC film. Besides, the peak at 1710 cm^{-1} (C=O stretching vibration of carboxyl groups) disappeared in the spectra of BP-based samples. Based on these results, it is safe to suggest that the BP, which contained oxygenated groups such as P-OH and P=O stemming from the partial oxidation of the few-layer BP (Wood *et al*. 2014), generated a strongly synergistic interaction with RC through intermolecular hydrogen bonds. In the spectra of the hybrid RC/GO samples, there were no noticeable changes in the band regions at 3400 cm^{-1} to 2800 cm^{-1} and 1650 cm^{-1} to 890 cm^{-1}. Meanwhile, the disappearance of the signal at 1710 cm^{-1} indicated that GO generated a certain effect on RC when mingled together. Meanwhile, the emergence of a new peak at 1745 cm^{-1} (C=O stretching vibration of ester groups) was associated with the possibility that some carboxyl groups of RC were chemically reacted with hydroxyls of GO forming

ester bonds during the cellulose dissolution. Compared with the above RC/GO samples, the spectra of cured RC-GO films showed obvious absorption bands that gave strong demonstration of acetylation: for instance, 1745 cm^{-1} corresponding to the ester C=O stretching mode, 1365 cm^{-1} was attributed to C-H bending, and 1240 cm^{-1} was assigned to the C-O stretching vibrations of carboxylic esters. The intensities of these peaks also increased with enhancing GO content, confirming that the number of ester groups increased through esterification between the additive and RC molecules. Additionally, the broad band of –OH groups at around 3340 cm^{-1} displayed a decreasing intensity with additional GO dosage due to the partial replacement of hydroxyls by ester groups. Upon a comparative analysis of RC/GO and RC-GO films, it was indicated that the curing treatment was an important factor for the formation of crosslinks between GO and RC during the esterification reaction.

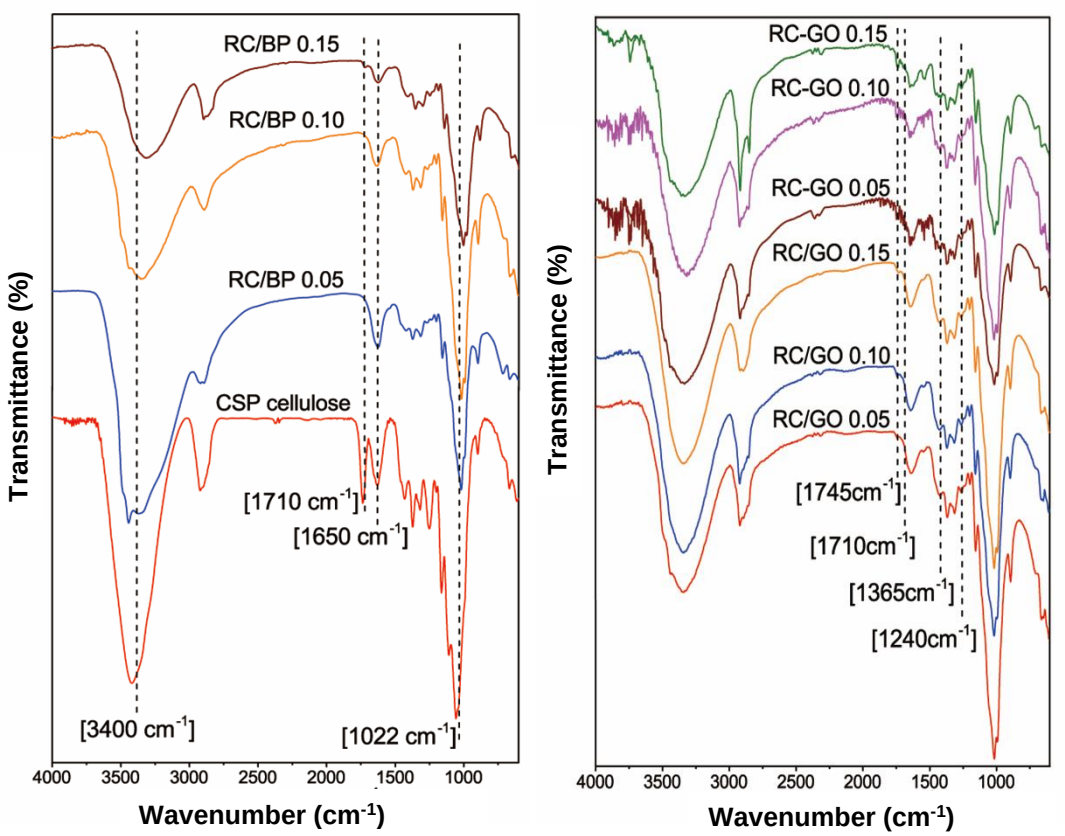

Fig. 2. FTIR spectra of CSP cellulose and RC-based films (RC/BP, RC/GO, and RC-GO samples) with various additive loadings

Morphology Observation

Photographs of the BP- and GO-based RC films with various additive contents are displayed in Fig. 3. The RC film without fillers showed a typical appearance of white translucency, while the colour of RC/BP composite films changed gradually from grey to brown with increased BP loading and their optical transmittance clearly declined. Regardless of the additive dosages, the GO-reinforced films were all black and opaque. Based on the above investigations, it was concluded that the homogeneous formation or mass distribution in the RC matrix was achieved by BP and GO as reinforced additives.

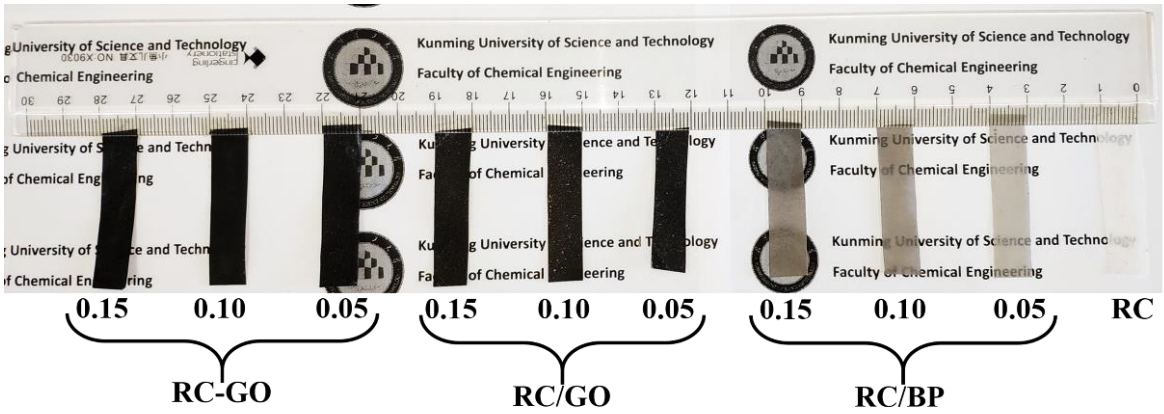

Fig. 3. Digital photographs of RC-GO, RC/GO, RC/BP, and RC films with the additive loadings of 0%, 0.05%, 0.10%, and 0.15% (wt%)

To further observe the influence of GO (or BP) addition on the top and fractured features of various treated films, a SEM analysis was conducted. Figure 4 reveals that the pure RC film had a rough and undulating surface, presumably composed of microparticles that agglomerated to each other and formed entangled structures. There was no agglomeration of the additives in the cellulose matrix as GO (or BP) dispersed uniformly throughout the film. The presence of these two additives led to the formation of compact morphologies in the surface of the composites, which might have been ascribed to the existence of strong interaction between the RC molecules and GO (or BP). The cross-sectional views of the different film samples are shown in the insert images of Fig. 4. It was evident that the morphological changes took place when the fillers were introduced into the RC matrix. The RC exhibited an uneven cross-sectional morphology with some cracks, which was reduced upon the introduction of the additives. The smoothness and compactness increased with the increased amounts of BP and GO. Additionally, the crosslinking method made the fracture surface of the obtained RC-GO films more tight and smooth. These well-bound surfaces and evenness were related to the indication of good reinforcement and uniform dispersion of the fillers in regenerated cellulose.

Crystalline and Thermogravimetric Analyses

The XRD patterns of the core cellulose, RC film, and GO- (or BP)-strengthened materials are shown in Fig. 5. Three typical peaks of the core cellulose located at 14.6°, 16.8°, and 22.8° were found, which corresponded to the diffraction of $(1\bar{1}0)$, (110), and (200) planes of cellulose-I, respectively (Reddy *et al.* 2017). The RC film prepared *via* the dissolution and coagulation in aqueous $ZnCl_2$ exhibited some new peaks at 2θ values of 11.2°, 18.6°, and 20.4°, revealing a characteristic cellulose-II structure (Yang *et al*. 2017). When cellulose was recrystallized during film forming, the growing of crystallites was incomplete, and thus the crystallinity was notably reduced. The diffraction peaks of the composite films (RC/GO and RC/BP samples) were similar to that of the pure RC, and the characteristic peaks corresponding to GO (or BP) were not detected. This could be ascribed to the insufficient amount of the additive in blend films and its uniform dispersion in the RC matrix (Ionita *et al*. 2016). However, the crystallinity indices of either RC/GO or RC/BP films were even lower than that of RC.

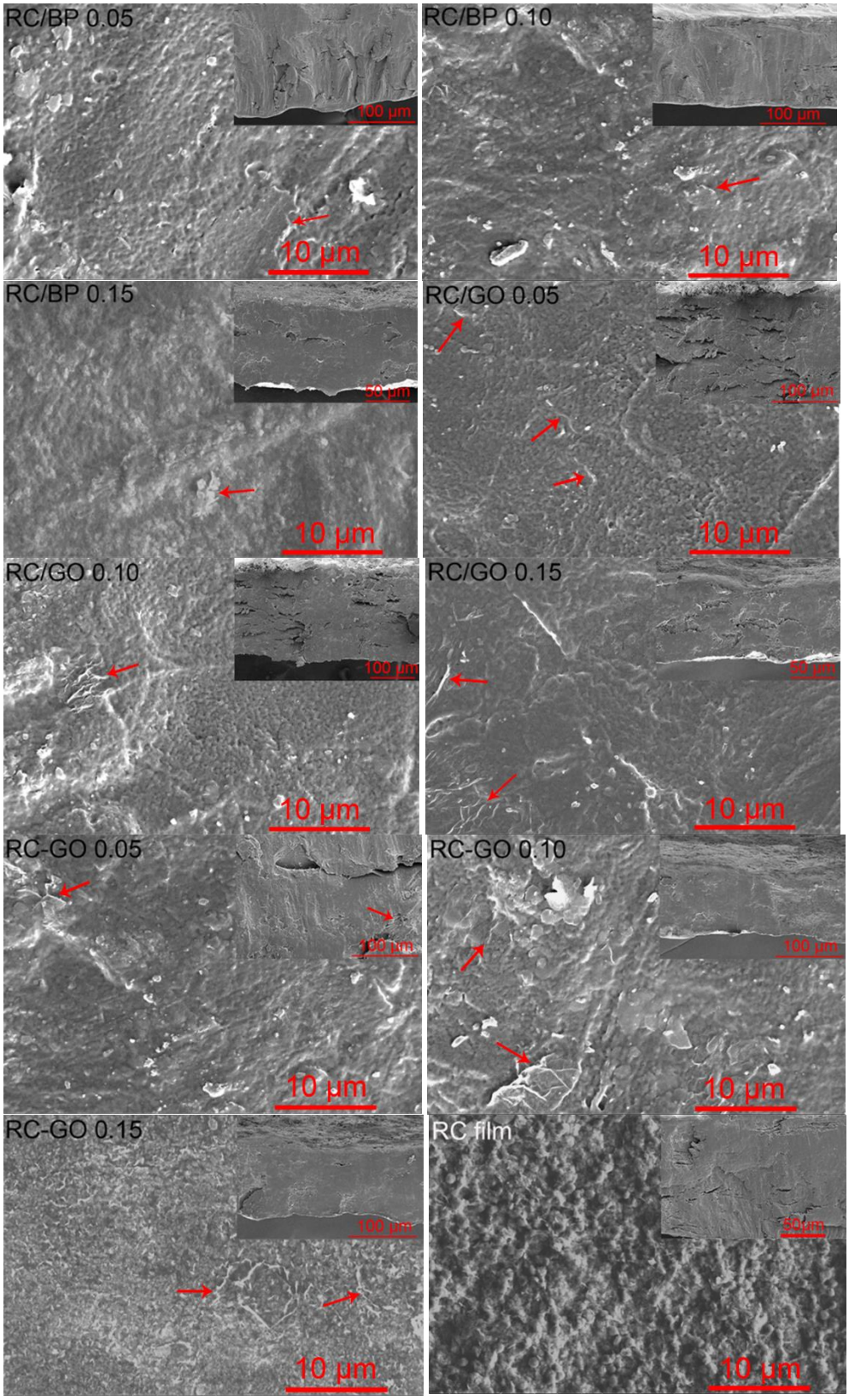

Fig. 4. SEM images of the top surfaces and the cross-sections (the inset images) of the RC nanocomposites incorporated with GO and BP nanosheets, respectively, at loadings of 0%, 0.05%, 0.10%, and 0.15% (wt%)

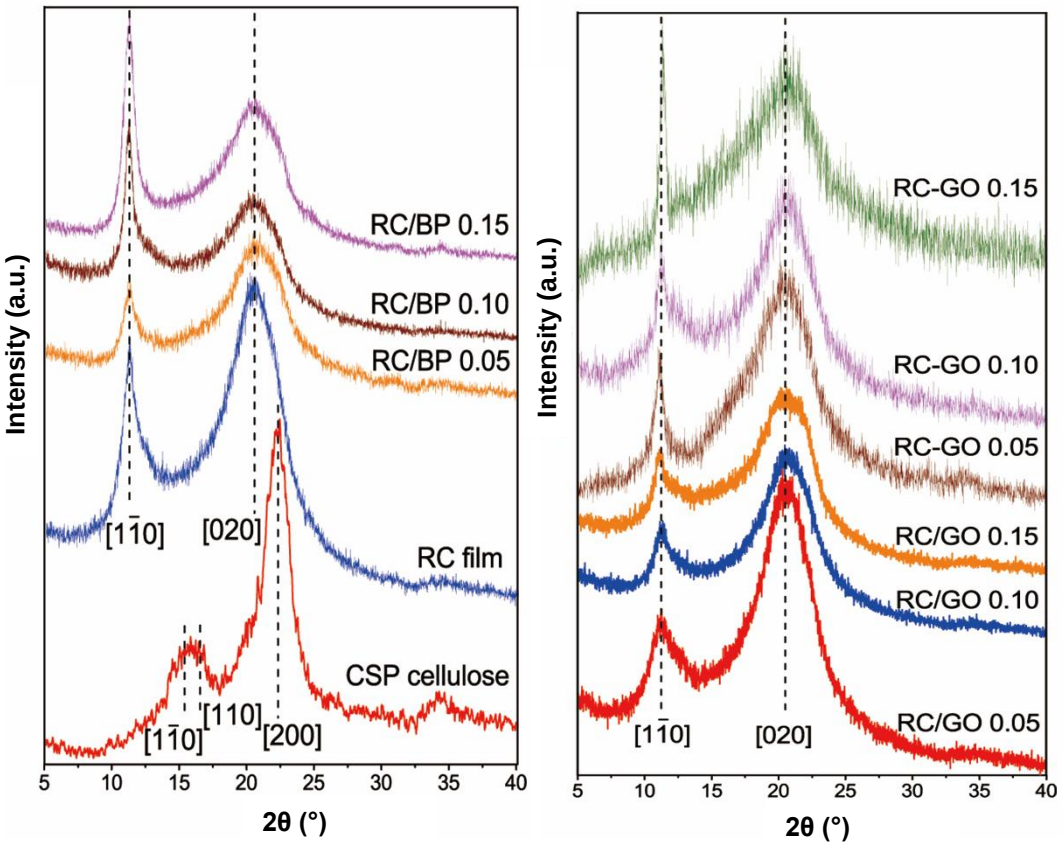

Fig. 5. XRD patterns of CSP cellulose, neat RC, RC/BP, RC/GO, and RC-GO blend films at various additive loadings

The lower crystallinity indices within the films hinted that the presence of GO (or BP) in the cellulose solution had an influence on the formation process of RC crystals, which generally originated from the disturbance by the fillers to the growing crystallites during cellulose regeneration. Similarly, RC-GO samples kept the same characteristic peaks in XRD spectra as the RC's, signifying that the crystalline structure of RC remained unchanged upon esterification with GO. Interestingly, the crystallinity indices of GO cross-linked films were close to (RC-GO 0.05) or somewhat higher (RC-GO 0.10 and RC-GO 0.15) than that of the RC sample, indicating the cellulose-II type cell parameters. This could be ascribed to the formation of a "quasi-crystal" structure in the amorphous region of cellulose after curing and cross-linking with GO (Yang *et al*. 2000).

To further understand the differences in thermal stability and degradable behaviours, various samples were heated from room temperature to 600 °C, and the recorded thermograms are depicted in Fig. 6a. For the corresponding DTG curves (Fig. 6b), the maximum decomposition temperature (T_{max}) of the RC film (295 °C) was lower than that of the untreated cellulose (350 °C). These findings distinctly demonstrated that the RC film had weaker thermal resistance in comparison to the original cellulose due to the fast degradation of these bio-polymeric molecules as well as the ruptures of inter/intramolecular hydrogen bonds of core cellulose during the dissolving process. For the composite films, the addition of GO or BP into the RC samples did not improve the thermal stability of the resulting film, and the increase in the filler content initiated the further decrease in thermal stability of the RC/GO (or BP) samples.

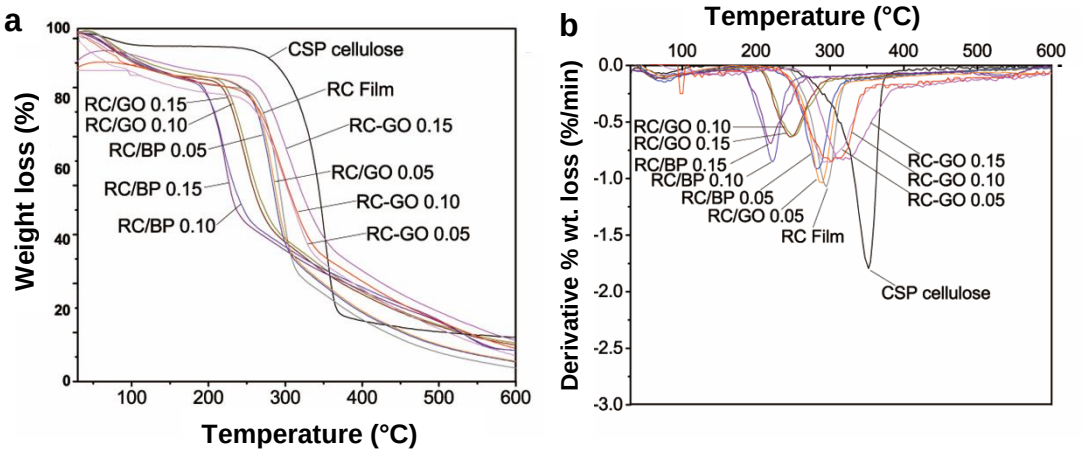

Fig. 6. Comparison of TGA (a) and DTG (b) curves for CSP cellulose, RC, RC/BP, RC/GO, and RC-GO functional films with a range of additive contents

Similar trends were reported in several studies (Ionita *et al*. 2016; Wei *et al*. 2017), explained by good thermal conductivities of both fillers that enhance the heat diffusion within polymer matrix and lead to fast decomposition of the composites. Under the same conditions of the additive loading, it was clear that the RC/BP film possessed a lower temperature of thermal decomposition than the RC/GO nanocomposite. This result might be due to one well-known problem that the few-layer BP nanosheet is more easily oxidized and decomposed in the air (Tian *et al*. 2018). Compared with RC/GO samples at the same loading levels, the initial degradation temperature (T_0) and T_{max} of cross-linked RC-GO films increased approximately 38 °C and 68 °C, respectively. This improvement was related to the formation of multiple cross-linked networks *via* ester linkages during the synthesis process of blend films. Moreover, it is worth noting that the values of T_0 and T_{max} for RC-GO 0.15 (253 °C and 318 °C, respectively) were higher than those of neat RC, hinting that the GO-crosslinked network in this study efficiently restricted the thermal decomposition of RC macromolecules. For the GO-incorporated films in comparison to the RC sample, the reduction of the mass loss at the first stage (below 150 °C) associated with water removal was observed. This could have been explained by the fact that GO physical interaction (or chemical crosslinking) with RC occurred *via* consumption of oxygen-containing groups leading to a smaller number of hydrophilic groups available to interact with the water molecules. Based on the TGA curve, the residual weight of the final degradation platform for the RC film was evidently lower than that of the original cellulose. This was because a degradation of cellulose chains happened during the dissolution process, as expected, leading to a comparatively lower DP value of the regenerated product. Meanwhile, as the additive GO (or BP) loading level enhanced, an increase in the final residual weight of the modified film was also identified.

Mechanical Performance

Figure 7a presents the tensile stress against the strain curves for the RC composite films doped with various contents of BP and GO as reinforcing additives. Compared with the pure RC film, it was noticed that introduction of BP and GO to the cellulose matrix *via* blending or crosslinking played an important role in the mechanical performance of the resultant films. Tensile strength, elongation at break, and Young's modulus, which are three critical mechanical properties for assessing films especially for packaging use, were characterized. The results are shown in Fig. 7b, c and d. The pure RC film could withstand

a stress of approximately 31.0 MPa with an elongation at break of 1.27% and Young's modulus of 5.66 GPa, due to the semi-rigid molecular chain properties of cellulose. When there was 0.15% GO (or BP) loading, the cellulose polymers displayed remarkably increased tensile strengths of 52.8 MPa (RC/BP), 77.6 MPa (RC/GO), and 89.9 MPa (RC-GO) which were 70.5%, 150.6%, and 190.2%, respectively, higher than that of RC film. At 0.05% GO (or BP) loading, the elongations at break for RC/BP, RC/GO, and RC-GO samples were approximately 5.68%, 4.47%, and 3.36%, respectively, which were more than 165% higher than that of the RC film. Meanwhile, the Young's modulus for the modified films showed a similar tendency as that for the tensile strength, which was an increase with the additive loading. It was clear from the above analysis that there was a general overall increase of the mechanical performance with the incorporation of GO and BP into the cellulose materials.

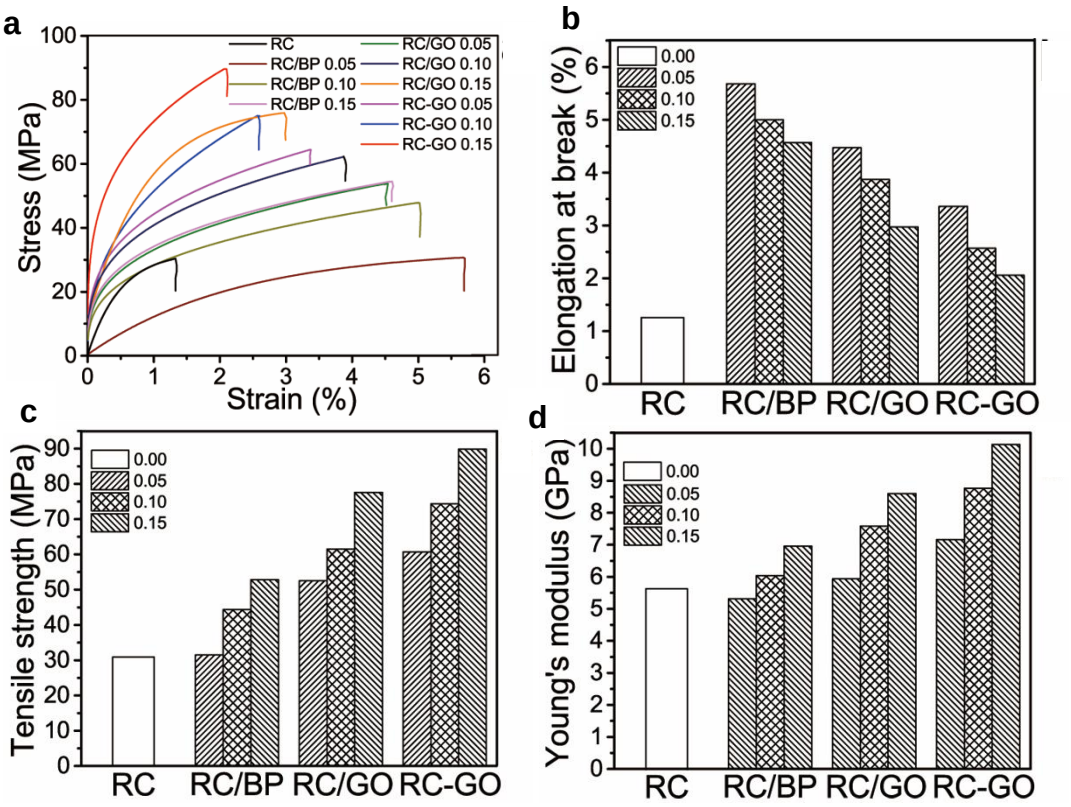

Fig. 7. Mechanical properties of RC film and the composites as a function of different additive loadings of BP and GO: stress-strain curves (a), elongation at break (b), tensile strength (c), and Young's modulus (d)

Improvements of the tensile strength and Young's modulus for the RC/GO and RC/BP samples with increasing filler contents indicated that GO and BP were well distributed and interacted with the RC matrix because of their comparatively low amounts (from 0.05% to 0.15%). The oxygen-containing groups on the surface and edges of exfoliated GO and BP nanosheets could be connected with RC molecular chains to form strong hydrogen bonds, which acted as interfacial load transfer regions between the RC and GO or BP (Gan *et al*. 2015). Thus, the increase of filler loading in the studied range had an obvious improvement on the mechanical properties.

Thus far, it has not been clear why the reinforcement behaviour of BP is quite weaker than that of GO, but this probably resulted from an easy deterioration property and

comparatively weak P-P bond strength of the few-layer BPs (Khandelwal *et al*. 2017). Under the same condition of loading, the improvements in the tensile strength and Young's modulus of GO-crosslinked RC films were optimal among the three kinds of functional samples. Compared with the preparation of RC/GO composites, the incorporation of GO induced the formation of additional cross-linking covalent bonds by dehydrating the mixture during a hot-curing process. These interactions are normally strong enough to act as the primary bonding mechanism between the GO sheets and RC matrix to reinforce the overall stability of the polymer structure and hence improve its mechanical strength.

In contrast, it was worth noting that the elongation at break of the composite films was higher than that of the RC sample. This improvement was attributed to the favourable interaction of exfoliated GO (or BP) with the cellulose matrix, leading to a certain increased flexibility of the RC polymer chains. However, a visible decrease of elongation at break was observed for all of the composites with increased GO (BP) content. This might be because under the condition of more additive loading, the interaction of the additives with RC matrix became tighter, which provided higher resistance to the movement of the cellulose chains. The fact that the greatest reduction of elongation at break occurred in the RC-GO films clearly suggested that the covalent cross-linking generated strong interfacial adhesion of cellulose with the GO nanosheet, leading to great restriction on the mobility of RC molecules. In comparison, RC/BP films displayed more favourable performance with a greater elongation at break, which was mainly ascribable to the flexible nature of few-layer BP *versus* GO sheets. In fact, phosphorene or few-layer BP has a puckered structure along the armchair direction and bilayer configuration along the zigzag direction. This structure leads to its superior ductile strength in the armchair direction and shows a rather unusual negative value of Poisson's ratio in an out-of-plane direction parallel to the pucker (Khandelwal *et al*. 2017).

Compared with the mechanical performances reported for other GO-reinforced nanocomposite films based on cellulose or its derivative matrices, the value of RC-GO 0.15 had the highest tensile strength and Young's modulus (89.88 MPa and 10.13 GPa, respectively) in this study. This result was distinctly higher than those of CC/4% GO (58.9 MPa for tensile strength and 4.86 GPa for Young's modulus) and CC-4% GO (50.9 MPa for tensile strength and 4.19 GPa for Young's modulus) prepared from conventional plant fibres as starting materials (Gan *et al*. 2015, 2017). Most notably, a small amount of GO (0.05 to 0.15%) loading considerably improved the physical properties of resultant films as discussed above, and these enhancements were more apparent than other recorded data (Wu *et al*. 2014; Phiri *et al*. 2018). These improvements might be largely dependent on a low-viscosity property of the $ZnCl_2$-dissolving parenchyma cellulose solution. The low viscosity facilitated the homogenous dispersion of GO nanosheets at the molecular level throughout this bio-matrix, and subsequently formed the strong connection between the additive and cellulose *via* hydrogen bonding and/or ester linkage during the dehydrated process. Meanwhile, the BP sheets could endure the stiff film materials with ideal break elongation in addition to acceptable strength properties. This experiment showed that an increase in the BP content had a lesser influence on the nanocomposite extensibility. In summary, inclusion of few-layer BP more remarkably improved the flexibility and ductility of the functional nanocomposite than the strength properties.

CONCLUSIONS

1. This study investigated the influence of graphene oxide (GO) and black phosphorene (BP) as additives on physical properties of regenerated cellulose (RC) films prepared from low-cost agricultural residue of corn stalk pith. The presence of the additive within the RC polymer matrix was confirmed by FTIR and SEM. Crystalline structure of RC and its composite films was proved to be cellulose II by XRD. A TG analysis showed that the increase of the additive loading caused an enhancement of residual weight at the final degradation stage.
2. A considerable improvement in terms of the maximum degradation temperature was observed for the cross-linked sample RC-GO 0.15, which exhibited an increase of 23 °C as compared with the pure RC film. Apparently, inorganic additive-modified RC films were successfully prepared with noticeable improvement of mechanical properties.
3. The overall results suggested that agro-waste parenchyma cells from corn stalk could be considered as a future source of feedstock for the cellulose regeneration and the mixture of GO and BP even with small amounts into this RC matrix play a critical role in enhancing the performances of CSP composite films.

ACKNOWLEDGMENTS

This work was financially supported by the National Natural Science Foundation of China (51963012), the Key Laboratory of Pulp and Paper Science and Technology of Ministry of Education/Shandong Province of China (KF201808), the Science Research Foundation Project of Yunnan Municipal Education Commission (2018js027), and the KMUST Scientific Research Foundation for the Introduction of Talent (KKSY201605058).

REFERENCE CITED

Ammar, A., Al-Enizi, A. M., AlMaadeed, M. A., and Karim, A. (2016). "Influence of graphene oxide on mechanical, morphological, barrier, and electrical properties of polymer membranes," *Arab. J. Chem* 9(2), 274-286. DOI: 10.1016/j.arabjc.2015.07.006

ASTM D882-97 (1999). "Standard test method for tensile properties of thin plastic sheeting," ASTM International, West Conshohocken, PA, USA.

Fan, T., Zhao, Z., Zhou, J., Li, L., Liu, Y., and Lu, M. (2018). "Fabrication of magnetic cotton fabrics using surface micro-dissolving technology in $ZnCl_2$ aqueous solution," *Cellulose* 25(2), 1437-1447. DOI: 10.1007/s10570-017-1623-0

Fu, F., Li, L., Liu, L., Cai, J., Zhang, Y., Zhou, J., and Zhang, L. (2015). "Construction of cellulose based ZnO nanocomposite films with antibacterial properties through one-step coagulation," *ACS Appl. Mater. Inter.* 7(4), 2597-2606. DOI: 10.1021/am507639b

Gan, S., Zakaria, S., Chia, C. H., Chen, R. S., and Jeyalaldeen, N. (2015). "Physico-mechanical properties of a microwave-irradiated kenaf carbamate/graphene oxide membrane," *Cellulose* 22(6), 3851-3863. DOI: 10.1007/s10570-015-0749-1

Gan, S., Zakaria, S., and Jaafar, S. N. S. (2017). "Enhanced mechanical properties of hydrothermal carbamated cellulose nanocomposite film reinforced with graphene oxide," *Carbohyd. Polym.* 172, 284-293. DOI: 10.1016/j.carbpol.2017.05.056

Gao, X., Chen, K. L., Zhang, H., Peng, L. C., and Liu, Q. X. (2014). "Isolation and characterization of cellulose obtained from bagasse pith by oxygen-containing agents," *BioResources* 9(3), 4094-4107. DOI: 10.15376/biores.9.3.4094-4107

Gao, X., Zhang, H., Chen, K. L., Zhou, J. L., and Liu, Q. X. (2018). "Removal of heavy metal and sulfate ions by cellulose derivative-based biosorbents," *Cellulose* 25(4), 2531-2545. DOI: 10.1007/s10570-018-1690-x

Garavand, F., Rouhi, M., Razavi, S. H., Cacciotti, I., and Mohammadi, R. (2017). "Improving the integrity of natural biopolymer films used in food packaging by crosslinking approach: A review," *Int. J. Biol. Macromol.* 104, 687-707. DOI: 10.1016/j.ijbiomac.2017.06.093

Grinshpan, D. D., Lushchik, L. G., Tsygankova, N. G., Voronkov, V. G., Irklei, V. M., and Chegolya, A. S. (1989). "Process of preparing hydrocellulose fibres and films from aqueous solutions of cellulose in zinc chloride," *Fibre Chem.* 20(6), 365-369. DOI: 10.1007/BF00547137

Hanlon, D., Backes, C., Doherty, E., Cucinotta, C. S., Berner, N. C., Boland, C., Lee, K., Harvey, A., Lynch, P., and Gholamvand, Z. (2015). "Liquid exfoliation of solvent-stabilized few-layer black phosphorus for applications beyond electronics," *Nat. Commun.* 6, Article Number 8563. DOI: 10.1038/ncomms9563

Ionita, M., Crica, L. E., Voicu, S. I., Pandele, A. M., and Iovu, H. (2016). "Fabrication of cellulose triacetate/graphene oxide porous membrane," *Polym. Adv. Technol.* 27(3), 350-357. DOI: 10.1002/pat.3646

Khandelwal, A., Mani, K., Karigerasi, M. H., and Lahiri, I. (2017). "Phosphorene-the two-dimensional black phosphorous: Properties, synthesis and applications," *Mat. Sci. Eng. B* 221, 17-34. DOI: 10.1016/j.mseb.2017.03.011

Lv, J. S., Liu, X. Y., Xu, J. X., Deng, Y. F., Wu, Z., Wang, Y. M., Fan, M. Y., and Xu, H. (2013). 'Preparation and properties of adsorption materials from corn stalks core when used for enzyme immobilization and the subsequent activities of the adsorbed enzymes," *Ind. Crop. Prod.* 50, 787-796. DOI: 10.1016/j.indcrop.2013.08.068

Phiri, J., Johansson, L. S., Gane, P., and Maloney, T. (2018). "A comparative study of mechanical, thermal and electrical properties of graphene-, graphene oxide- and reduced graphene oxide-doped microfibrillated cellulose nanocomposites," *Compos. Part B* 147, 104-113. DOI: 10.1016/j.compositesb.2018.04.018

Reddy, K. O., Maheswari, C. U., Dhlamini, M. S., Mothudi, B. M., Zhang, J., Zhang, J., Nagarajan, R., and Rajulu, A. V. (2017). "Preparation and characterization of regenerated cellulose films using borassus fruit fibers and an ionic liquid," *Carbohyd. Polym.* 160, 203-211. DOI: 10.1016/j.carbpol.2016.12.051

Schestakow, M., Karadagli, I., and Ratke, L. (2016). "Cellulose aerogels prepared from an aqueous zinc chloride salt hydrate melt," *Carbohyd. Polym.* 137, 642-649. DOI: 10.1016/j.carbpol.2015.10.097

Sen, S., Losey, B. P., Gordon, E. E., Argyropoulos, D. S., and Martin, J. D. (2016). "Ionic liquid character of zinc chloride hydrates define solvent characteristics that

afford the solubility of cellulose," *J. Phys. Chem. B* 120(6), 1134-1141. DOI: 10.1021/acs.jpcb.5b11400

Tian, B., Tian, B., Smith, B., Scott, M. C., Lei, Q., Hua, R., Tian, Y., and Liu, Y. (2018). "Facile bottom-up synthesis of partially oxidized black phosphorus nanosheets as metal-free photocatalyst for hydrogen evolution," *PNAS* 21(17), 1-6. DOI: 10.1073/pnas.1800069115

Wei, X., Huang, T., Yang, J. H., Zhang, N., Wang, Y., and Zhou, Z. W. (2017). "Green synthesis of hybrid graphene oxide/microcrystalline cellulose aerogels and their use as superabsorbents," *J. Hazard. Mater.* 335, 28-38. DOI: 10.1016/j.jhazmat.2017.04.030

Wood, J. D., Wells, S. A., Jariwala, D., Chen, K. S., Cho, E. K., Sangwan, V. K., Liu, X., Lauhon, L. J., Marks, T. J., and Hersam, M. C. (2014). "Effective passivation of exfoliated black phosphorus transistors against ambient degradation," *Nano Lett.* 14(12), 6964-6970. DOI: 10.1021/nl5032293

Wu, Y., Li, W., Zhang, X., Li, B., Luo, X., and Liu, S. (2014). "Clarification of GO acted as a barrier against the crack propagation of the cellulose composite films," *Compos. Sci. Technol.* 104, 52-58. DOI: 10.1016/j.compscitech.2014.09.004

Xu, Q., Chen, C., Rosswurm, K., Yao, T., and Janaswamy, S. (2016). "A facile route to prepare cellulose-based films," *Carbohyd. Polym.* 149, 274-281. DOI: 10.1016/j.carbpol.2016.04.114

Yang, G., Zhang, L., Peng, T., and Zhong, W. (2000). "Effects of Ca^{2+} bridge cross-linking on structure and pervaporation of cellulose/alginate blend membranes," *J. Membrane Sci.* 175(1), 53-60. DOI: 10.1016/S0376-7388(00)00407-5

Yang, Y., Zhang, Y., Dawelbeit, A., Deng, Y., Lang, Y., and Yu, M. (2017). "Structure and properties of regenerated cellulose fibers from aqueous NaOH/thiourea/urea solution," *Cellulose* 24(10), 4123-4137. DOI: 10.1007/s10570-017-1418-3

Zhang, J., Wang, Y. H., Qu, Y. S., Wei, Q. Y., and Li, H. Q. (2018). "Effect of the organizational difference of corn stalk on hemicellulose extraction and enzymatic hydrolysis," *Ind. Crop. Prod.* 112, 698-704. DOI: 10.1016/j.indcrop.2018.01.007

Article submitted: June 13, 2019; Peer review completed: August 16, 2019; Revised version received: September 2, 2019; Accepted: September 5, 2019; Published: September 10, 2019.
DOI: 10.15376/biores.14.4.8455-8469